A transition from diagenesis to greenschist facies within a major Variscan fold/thrust complex in south-west England

T. J. PRIMMER*

Department of Geology, University of Bristol, Queen's Building, University Walk, Bristol BS8 1TR

ABSTRACT. The north coast of Cornwall, from Bude to Newquay, provides a continuous section through a major Variscan fold/thrust complex. Illite crystallinity studies have revealed a transition from diagenesis in the north to greenschist facies metamorphism in the south in the Upper Palaeozoic succession. More detailed studies of mineral assemblages in both metabasites and pelitic rocks support the regional pattern of metamorphism indicated by illite crystallinity, and show that locally in the Tintagel district, the grade of metamorphism may have reached middle to upper greenschist facies. An attempt to correlate the above data with temperatures (108–985 °C) derived from O-isotope geothermometers is made. Interpretation of the metamorphic data presented helps to emphasize the tectonic importance of the major structures seen in the fold/thrust complex.

KEYWORDS: diagenesis, greenschist facies, illite, Variscan, Cornwall, England.

THE geology of south-west England is dominated by a largely clastic sequence of Upper Palaeozoic sediments that has suffered a polyphase deformational history as a result of Variscan orogenic activity. In this context a study of the extent to which these sediments have been altered by burial and tectonism may help elucidate the complex pattern of structures in south-west England.

The coastal section between Newquay and Bude (fig. 1) has been chosen to demonstrate the degree of low-temperature alteration as it displays a continuous section through a major Variscan fold/thrust complex. Here the rocks show both the greatest range in age (Lower Devonian to Upper Carboniferous) and variability in structural style. Brazier *et al.* (1979) presented preliminary results from a study of illite crystallinity of samples from the north Cornwall coast. Their data suggest anchizone grade for Middle and Upper Devonian rocks in the Padstow area, epizone for Upper

* Present address: Department of Geology, Imperial College of Science and Technology, Prince Consort Road, London SW7 2BP.

Devonian and Lower Carboniferous rocks in the Tintagel area and lower grades, anchizone to diagenetic zone for Upper Carboniferous rocks to the north. Descriptions of greenschist facies mineral assemblages in the Tintagel area (Robinson and Read, 1981) support earlier observations (Tilley, 1925; Phillips, 1928) and confirm that the highest grade metamorphic effects occurred in that area. A more detailed study using similar techniques is made here and isotopic geothermometers are also used to provide more detailed information which is interpreted in the light of recent structural and tectonic syntheses.

Layer silicate mineralogy and crystallinity determinations. XRD analysis of 122 samples shows that throughout the Devonian slates the $< 2 \mu m$ phyllosilicate assemblage is dominated by a 10 Å illite/muscovite phase and chlorite with minor occurrences of pyrophyllite (fig. 2). Chlorite-free assemblages are found in black, Lower Carboniferous slates, but the greatest variety of assemblage is found in the Upper Carboniferous, Crackington and Bude Formations. The uniformity in mineralogy throughout rocks of Devonian age suggests that there is a low-temperature metamorphic influence, with rocks in the illite–chlorite zone of Velde (1977), and indicating that temperatures must have exceeded 200 °C. This contrasts sharply with the very rapid and localized changes in mineralogy seen in the Upper Carboniferous rocks, especially the Crackington Formation. Grainger and Witte (1981) have suggested that this is due primarily to variations in detrital input and later structural complication of the outcrop which have produced rapid variations between kaolinite-bearing and chlorite-bearing assemblages. The restricted occurrence of an expandable, mixed-layered phase similarly suggests that a control on detrital input has occurred. The ordered nature of the stratification, an IS rectorite-type (Bailey, 1982) with *c.* 50% illite interlayers, indicates that there
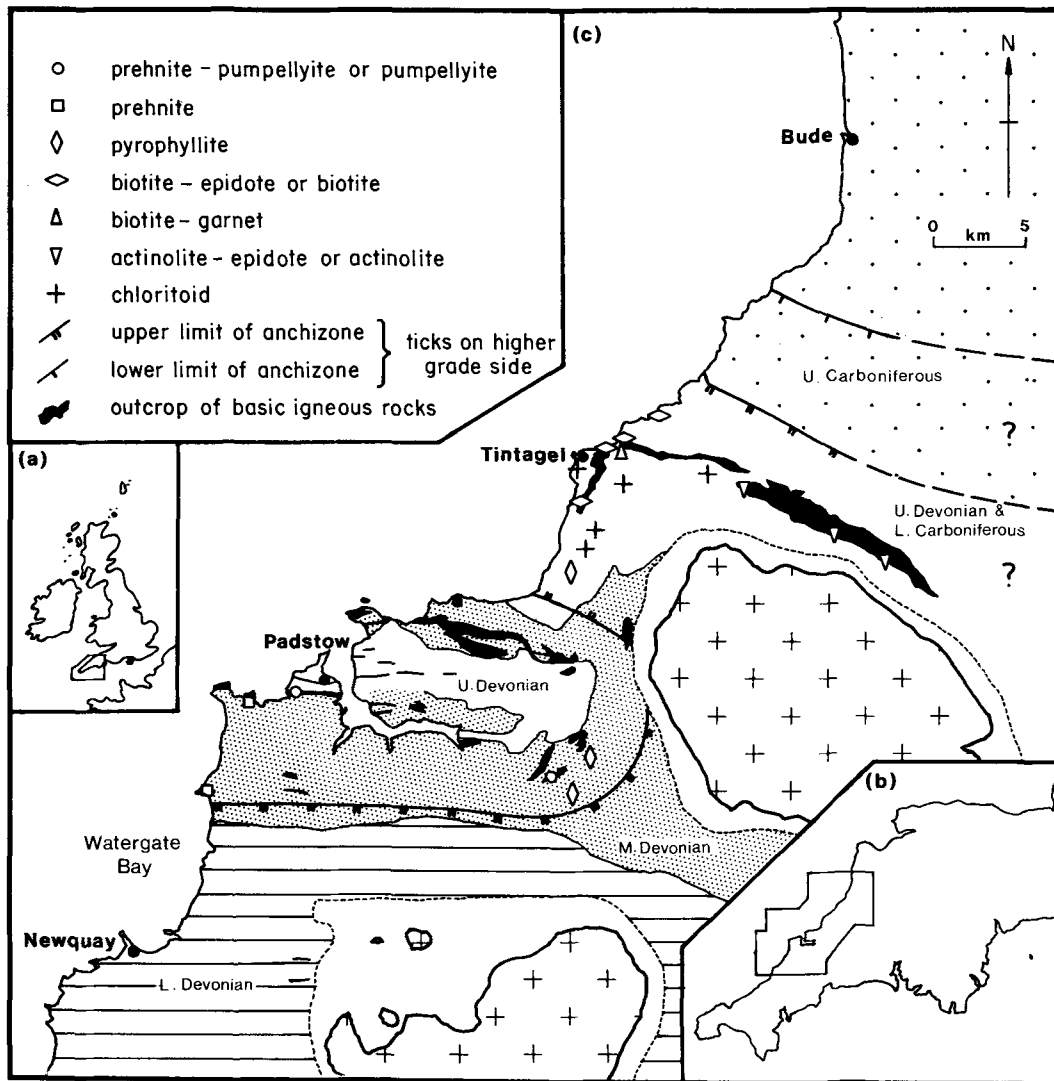
FIG. 1. Location of study area in south-west England summarizing the Upper Palaeozoic igneous and sedimentary outcrop, the distribution of illite crystallinity zones, and the occurrence of paragenetically important metamorphic mineral assemblages. The outcrop and extent of thermal metamorphic aureoles around the post orogenic granite cupolas are also illustrated.

must have been some form of modification of a detrital smectite-rich expandable precursor at temperatures in excess of *c.* 120 °C (Velde, 1977), but remaining below the upper stability limit of kaolinite.

The widespread acceptance of illite crystallinity as a measure of low-temperature metamorphism in argillaceous sediments (reviewed by Kisch, 1983), and the preliminary data obtained by Brazier *et al.* (1979) indicates that a detailed evaluation of crystallinity indices within the study area would yield more precise information on the degree of metamorphism. All determinations were made according to the techniques of Primmer (1983); both Weaver (sharpness) ratios and peak-width measurements were made on each sample and are listed in full in Primmer (1984). Weaver values range from 1.9 to 20.5 and peak-widths from 0.15 to 0.68° 2θ (Cu-$K\alpha$ radiation) covering the complete range from diagenesis to epizone metamorphism.

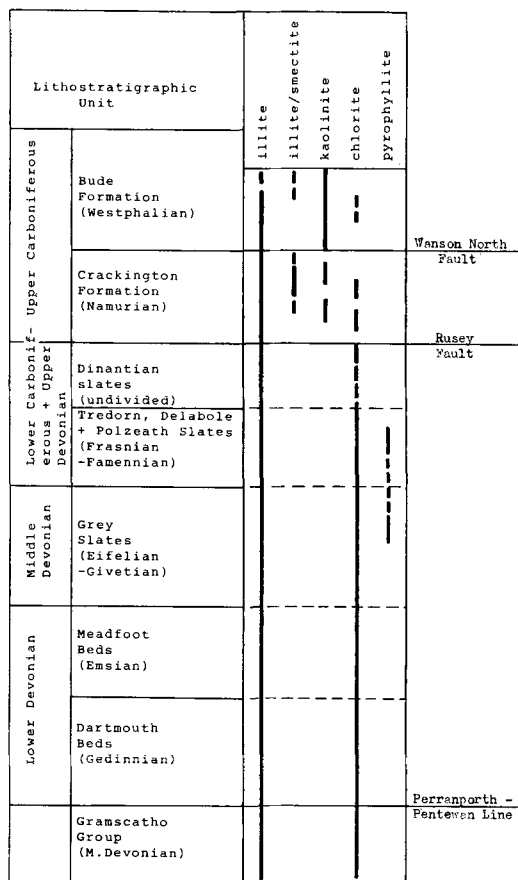| Lithostratigraphic Unit		illite	illite/smectite	kaolinite	chlorite	pyrophyllite
Upper Carboniferous	Bude Formation (Westphalian)					
	Crackington Formation (Namurian)					
Lower Carbonif.+ Upper Devonian	Dinantian slates (undivided)					
	Tredorn, Delabole + Polzeath Slates (Frasnian -Famennian)					
Middle Devonian	Grey Slates (Eifelian -Givetian)					
Lower Devonian	Meadfoot Beds (Emsian)					
	Dartmouth Beds (Gedinnian)					
	Gramscatho Group (M.Devonian)					

(Wanson North Fault; Rusey Fault; Perranporth – Pentewan Line)

FIG. 2. Distribution of phyllosilicate minerals in < 2 μm size fraction.

Fig. 1 shows the geographical distribution of crystallinity zones, based on the following boundary values.

Index	Diagenetic zone	Anchizone	Epizone
Weaver (Weaver, 1960)	< 2.3	2.3–12.1	> 12.1
Peak-width (° 2θ Cu-$K\alpha$) (Kisch, 1980)	> 0.38	0.21–0.38	< 0.21

The variation in illite crystallinity through the section studied is illustrated in fig. 3, where peak-width values of 88 samples along the coastal section are plotted.

The gradual transition between epizone and anchizone grades in the Devonian rocks between Newquay and Tintagel and similarly between the anchizone and diagenetic zone in the Upper Carboniferous from the Rusey fault to Bude are illustrated in fig. 3. A much more abrupt change

coincident with the Rusey fault is also identified. To the south the Lower Carboniferous (Selwood et al., 1984) are epizone grade slates while the Upper Carboniferous to the north are lower anchizone. Clearly, the sharp transition in metamorphic grade emphasizes the importance of this structural feature. In the same context, a major composite D2/D3 east-west antiformal structure (the Dartmouth antiform of Hobson, 1976) which outcrops on the north Cornwall coast in Watergate Bay, just north of Newquay, influences the exposure of epizone-grade slates. The later phases of folding have brought these higher grade slates up from depth after the epizone grades of metamorphism developed at the lower structural level.

Mineral paragenesis of metabasites and Tintagel slates. Two broad belts of igneous rocks have been identified in the region (Floyd, 1982); a northern belt consisting mainly of lavas, tuffs, and agglomerates of Upper Devonian and Lower Carboniferous age, stretches from the coast at Tintagel eastwards around the northern flank of Bodmin Moor. The southern belt, comprising both lavas and associated high-level dykes and sills, outcrops on the coast near Padstow and in a broad easterly tract towards the southern flank of Bodmin Moor.

Contrasting metamorphic mineral assemblages have been identified in each belt, these are summarized below and in fig. 1.

Northern belt:
  chlorite-albite-biotite ± epidote ± calcite
  chlorite-albite-actinolite ± epidote

Southern belt:
  chlorite-albite ± epidote ± calcite
  chlorite-albite-pumpellyite ± prehnite ± epidote
  chlorite-albite-prehnite ± epidote

The determination of the mineral chemistry of each of these phases was made by electron microprobe analysis (analyses are listed in full in Primmer, 1984).

Floyd and Rowbotham (1982) have reported prehnite-pumpellyite-bearing assemblages at Trevone near Padstow, but examination on a wider scale throughout the district reveals that the non-diagnostic chlorite-albite ± calcite type assemblage is more typical. Larger intrusive bodies only rarely contain abundant pumpellyite (with or without prehnite), similarly, prehnite bearing veins are found without pumpellyite in similar locations. However, in all cases where there is abundant calcite (usually developed near the margins of the igneous bodies) no Ca-Al hydrosilicates are developed. The pumpellyite analysed in this study is of the Fe-rich variety (fig. 4) and in thin section shows a strong green-blue β absorption in the
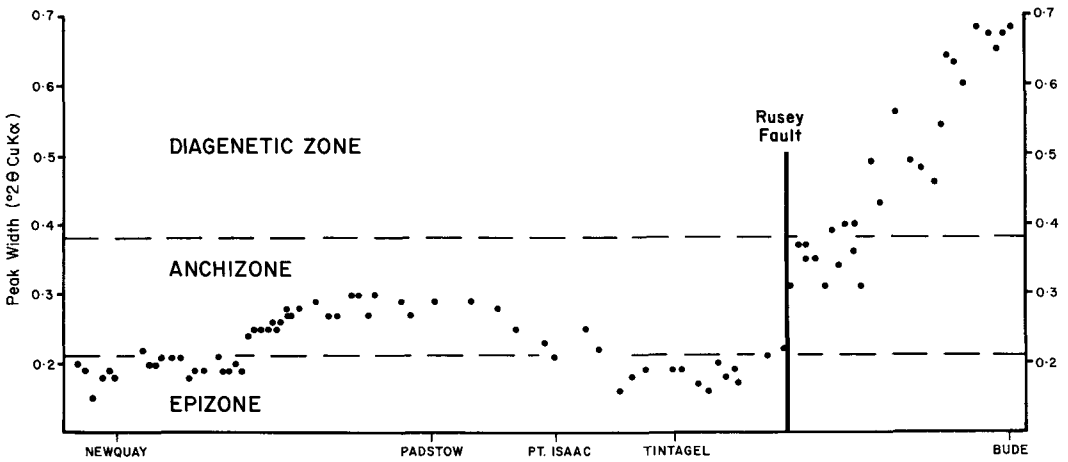
FIG. 3. Variation in illite crystallinity (expressed in peak-width values) along the coast representing a section through the fold/thrust complex.
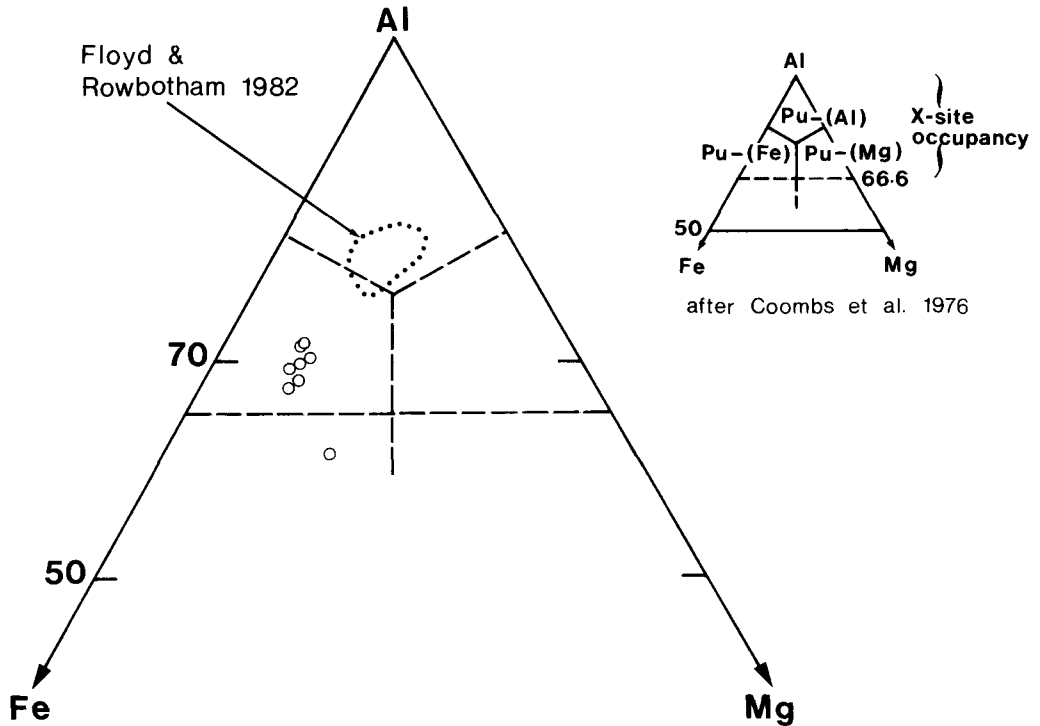

FIG. 4. Pumpellyite composition from this study and Floyd and Rowbotham (1982) on a Fe*:Al:Mg diagram, fields divided according to Coombs et al., 1976 (inset), on the basis of the x-site occupancy in the unit formula. Fe*: total iron as Fe^{3+}.

pleochroic scheme, typical of Fe-rich pumpellyites found in zeolite and prehnite-pumpellyite facies terrain (Liou, 1979). This is in direct contrast to data presented by Floyd and Rowbotham (1982), who described an Al-rich variety of pumpellyite in their study (fig. 4), which is usually characteristic of pumpellyite–actinolite facies metamorphism (Coombs et al., 1976). Offler et al. (1981) related variations in pumpellyite composition to the degree of alteration of primary Fe–Ti oxides and suggested that a progressive degradation of mafic igneous phases releases Fe for incorporation into the crystallizing pumpellyite during metamorphism. Floyd and Rowbotham (1982) commented that the specimens they studied contained abundant, little-altered mafic igneous phases (particularly Fe-oxides); however, the Fe-rich pumpellyite analysed in this study occurs in specimens where all the primary Fe–Ti oxides have been completely pseudomorphed by sphene. Thus the Fe-rich pumpellyite is more indicative of the (equilibrium) metamorphic conditions that prevailed in the southern belt (i.e. prehnite–pumpellyite facies).

Chlorite–albite type assemblages similarly dominate the metabasites in the Tintagel area, although biotite- and actinolite-bearing assemblages here clearly indicate that the greenschist facies was reached throughout the northern belt as suggested by Robinson and Read (1981). The only significant chemical variation in the mineral chemistry is in Mg and Fe^{2+}, with mineral Mg/Fe^{2+} ratios controlled by bulk rock compositions. Associated slates show a Mn-rich garnet–biotite assemblage. Analysis of the mineral chemistry using the equilibrium Mg/Fe^{2+} exchange relationship between co-existing garnet and biotite has allowed application of the solid solution garnet–biotite geothermometer of Pigage and Greenwood (1982), modified after Ferry and Spear (1978). Temperatures in the order of 450 ($\pm$ 50) °C have been calculated (Primmer, 1984) for three mineral pairs within one sample. Textural relationships show that these minerals crystallized during a post-kinematic (M2) phase of metamorphism, suggesting that temperatures reached mid to upper greenschist facies after the initial epizone M1/D1 phase recorded by illite crystallinity.

Chloritoid-bearing assemblages have long been identified within the Upper Devonian slates of the Tintagel district (Hutchings, 1889). Detailed study of the petrography and mineral chemistry shows that chloritoid–muscovite–chlorite assemblages represent 'high-Al limiting' assemblages (Guidotti and Sassi, 1976), which are controlled by bulk rock composition (fig. 5). Such Al-rich parageneses may persist to higher temperatures, with crystallization of porphyroblastic phases during M2, at the expense

of more normal index minerals such as biotite and garnet up to the stability limit of co-existing muscovite and chlorite (c. 500 °C).

Oxygen isotope geothermometry. Another method of characterizing the temperature of metamorphism is by the application of oxygen isotope geothermometry. As there are no paragenetically useful mineral assemblages or basic igneous rock outcrops in the area between Bude and Tintagel, this section was used in an attempt to correlate the crystallinity zones with absolute temperature. $\delta^{18}O$ values (in ‰ relative to SMOW) were obtained using the techniques of Eslinger et al. (1979) on different phyllosilicate-rich mineral size fractions and also from a $< 2 \mu m$ quartz separate (isolated by the method of Syers et al., 1968). Table I lists the $\delta^{18}O$ values obtained. Chlorite was removed from samples by treatment with 1M HCl at 80 °C; the analysed residue thus representing the $\delta^{18}O$ value of the illite. A $\delta^{18}O$ value for the dissolved chlorite was then determined by a simple mass balance calculation. With samples containing kaolinite, however, removal of the kaolinite is not possible without affecting the illite present. $\delta^{18}O$ values for the illite in these phyllosilicate fractions were determined by adjusting the whole rock value relative to the amount of kaolinite present (determined by the method of Johns and Kurzweil, 1979) and by assuming an average value of 19.5 ‰ (SMOW) for the $\delta^{18}O$ of the detrital kaolinite (Milliken et al., 1981; McMurty et al., 1983).

Temperatures for quartz–illite pairs were calculated from the empirically calibrated geothermometer of Eslinger and Savin (1973)

$$1000 \ln \alpha_{quartz-illite} = 0.95(10^6 T^{-2}) + 0.88.$$

An approximation for a quartz–chlorite geothermometer can be obtained from published literature, i.e.

$$\Delta_{quartz-chlorite} = 0.59 \Delta_{quartz-ilmenite}$$
(Wenner and Taylor, 1971)

$$\Delta_{quartz-muscovite} = 0.35 \Delta_{quartz-ilmenite}$$
(Taylor and Coleman, 1968)

using calibrated mineral–water fractionation relationships.

$$1000 \ln \alpha_{quartz-water} = 3.35(10^6 T^{-2}) - 3.31$$
(Matsuhia et al., 1979)

$$1000 \ln \alpha_{muscovite-water} = 2.38(10^6 T^{-2}) - 3.89$$
(O'Neil and Taylor, 1969)

gives the approximation,

$$\Delta_{quartz-chlorite} \approx 1.62(10^6 T^{-2}) + 0.98$$
(where $\Delta_{A-B} = \delta_A - \delta_B$).

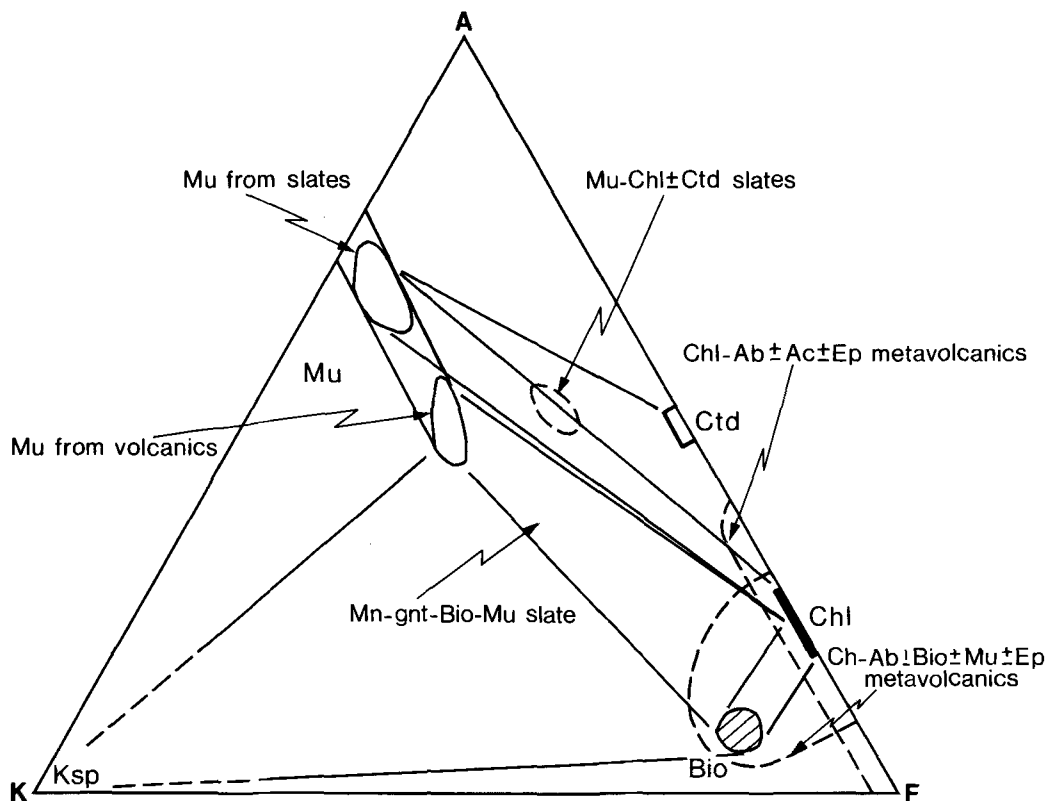Temperatures derived from both geothermometers are given in Table I and the relationship

FIG. 5. AKF diagram representing metamorphic assemblages found in the Tintagel district and northern belt of metabasites. Solid fields represent the compositional range of the minerals indicated. Broken fields (and dot) represent the range of bulk composition for the assemblages indicated. (Abbreviations: Mu muscovite; Chl chlorite; Ctd chloritoid; Bio biotite; Ep epidote; Ac actinolite; Ab albite; Gnt garnet; Ksp K feldspar.)

between the calculated temperatures and the crystallinity zones is illustrated in fig. 6. It is immediately apparent that some of the calculated temperatures represent non-equilibrated isotopic systems, i.e. illite in sample 1, chlorite in sample 67 and quartz in sample 38 are not in isotopic equilibrium with other minerals in the assemblage. In the case of sample 67 it is thought that the chlorite is detrital and has not re-equilibrated during low-temperature metamorphism, whereas the $\delta^{18}O$ quartz value in sample 38 is the lowest recorded and may well be a result of contamination during quartz isolation or isotopic fractionation during oxygen extraction. Petrographic evidence in the Tintagel district shows that there was a late phase of retrograde metamorphism with an accompanying growth of fine-grained phyllosilicate minerals pseudomorphing earlier porphyroblastic (M2) phases. This may be the cause of the more enriched $\delta^{18}O$ value for the illite in sample 1, there being a mixture

of prograde (relatively depleted) and retrograde (more enriched) illite in the fraction analysed.

The best indication that isotopic equilibrium was at least approached in some samples is shown by the ternary illite–chlorite–quartz system in sample 28. A fairly consistent trend of isotopic temperatures in the different size fractions can be seen. Two main groups of temperatures can be identified:

1. Temperatures < 200 °C from north of the Rusey fault, indicating predominantly diagenetic zone/sub-greenschist facies temperatures, although the well-defined transition from diagenetic grades through to anchizone from north to south indicated by illite crystallinity is not recorded by the isotopically derived temperatures.

2. Temperatures > 300 °C from one quartz-illite sample south of the Rusey fault along with other quartz–chlorite temperatures approaching 300 °C shows that metamorphic temperatures were clearly higher, although only temperatures in

Table I. Oxygen isotope geothermometry

Sample		$\delta^{18}O$ [1]	%Kao [2]	%Chl [3]	$\delta^{18}O$ illite [4]	$\delta^{18}O$ chlorite [5]	$\delta^{18}O$ quartz [6]	T°C (qz-ill)	T°C (qz-chl)
43	2-1μm	13.60	13	–	12.70	–	19.30	152	–
	1-0.5μm	13.04	11	–	12.27	–	,,	135	–
	<0.5μm	12.06	8	–	11.43	–	,,	108	–
51	2-1μm	14.31	11	–	13.67	–	20.35	132	–
	1-0.5μm	13.82	7	–	13.43	–	,,	124	–
	<0.5μm	13.98	3	–	13.79	–	,,	136	–
53	2-1μm	14.38	8	–	13.94	–	18.59	229	–
55	2-1μm	14.46	15	–	13.58	–	19.46	163	–
67	2-1μm	13.38	–	25	15.24	7.71	21.15	162	*
	1-0.5μm	13.65	–	24	15.48	7.76	,,	172	*
	<0.5μm	12.44	–	28	14.31	7.53	,,	126	*
38	2-1μm	14.68	6	–	14.35	–	17.95	318	–
36	2-1μm	14.11	–	–	14.11	–	19.30	197	–
	1-0.5μm	13.55	–	–	13.55	–	,,	169	–
	<0.5μm	13.38	–	–	13.38	–	,,	161	–
1	2-1μm	15.38	–	26	16.57	11.92	18.05	(985)	287
	1-0.5μm	14.98	–	30	16.27	11.91	,,	(754)	287
28	2-1μm	15.05	–	34	15.59	14.00	18.73	377	384
	1-0.5μm	14.57	–	29	15.24	12.91	,,	331	306
	<0.5μm	14.04	–	51	15.16	12.98	,,	321	310

1. Measured on whole size fraction (all δ values quoted in ‰ relative to SMOW)

2. % kaolinite in size fraction determined according to the method of Johns and Kurzweil (1979)

3. % material lost after HCl treatment.

4. Kaolinite bearing assemblages: $\delta^{18}O$ adjusted by estimating $\delta^{18}O$ kaolinite = 19.5%

5. Calculated value from mass balance.

6. Measured on <2μm portion of quartz isolated from sample.

*Temperature not calculated; chlorite not in isotopic equilibrium with quartz.

Brackets indicate temperatures influenced by contribution from retrograde illite.

excess of 375 °C unequivocally indicate greenschist facies conditions were reached.

Temperatures obtained throughout this study would appear to be lower than expected. This may well be a function of the mineral geothermometers used in that they are derived from the isotopic characteristics of essentially open systems, e.g. the quartz–illite geothermometer of Eslinger and Savin (1973) was calibrated from data from the Ohaki–Broadlands geothermal area in New Zealand. Similarly, the quartz–chlorite fractionation relationships rely heavily on data derived from the serpentinization of ultrabasic rocks (Wenner and Taylor, 1971). These systems are rather dissimilar to the closed diagenetic/low-temperature metamorphic regime described here; consequently it would be presumptious to interpret the temperatures obtained too literally. However, the trend in the data presented is encouraging and, with further isotopic studies of this kind in similar terrains, a more refined series of geothermometers for low-temperature metamorphism may produce more realistic temperatures. Of prime importance is that the type of mechanism involved in the crystallization of phyllosilicate lattices and its role in the fractionation of oxygen isotopes should be identified. A full analysis of these problems is beyond the scope of this discussion but has been touched upon by Yeh and Savin (1977). A pointer for future study is to explain the fairly consistent (albeit small) trend to more depleted $\delta^{18}O$ values in the finer size fractions in all the phyllosilicate samples studied irrespective of grade. This may be a feature of the isotopic fractionation process or merely the indication of the susceptibility of finer size fractions to chemical (and consequently isotopic) modification during the pretreatment of samples (Eslinger et al., 1979) relative to the coarser fractions.

However, it is apparent that there is no significant isotope readjustment under either higher
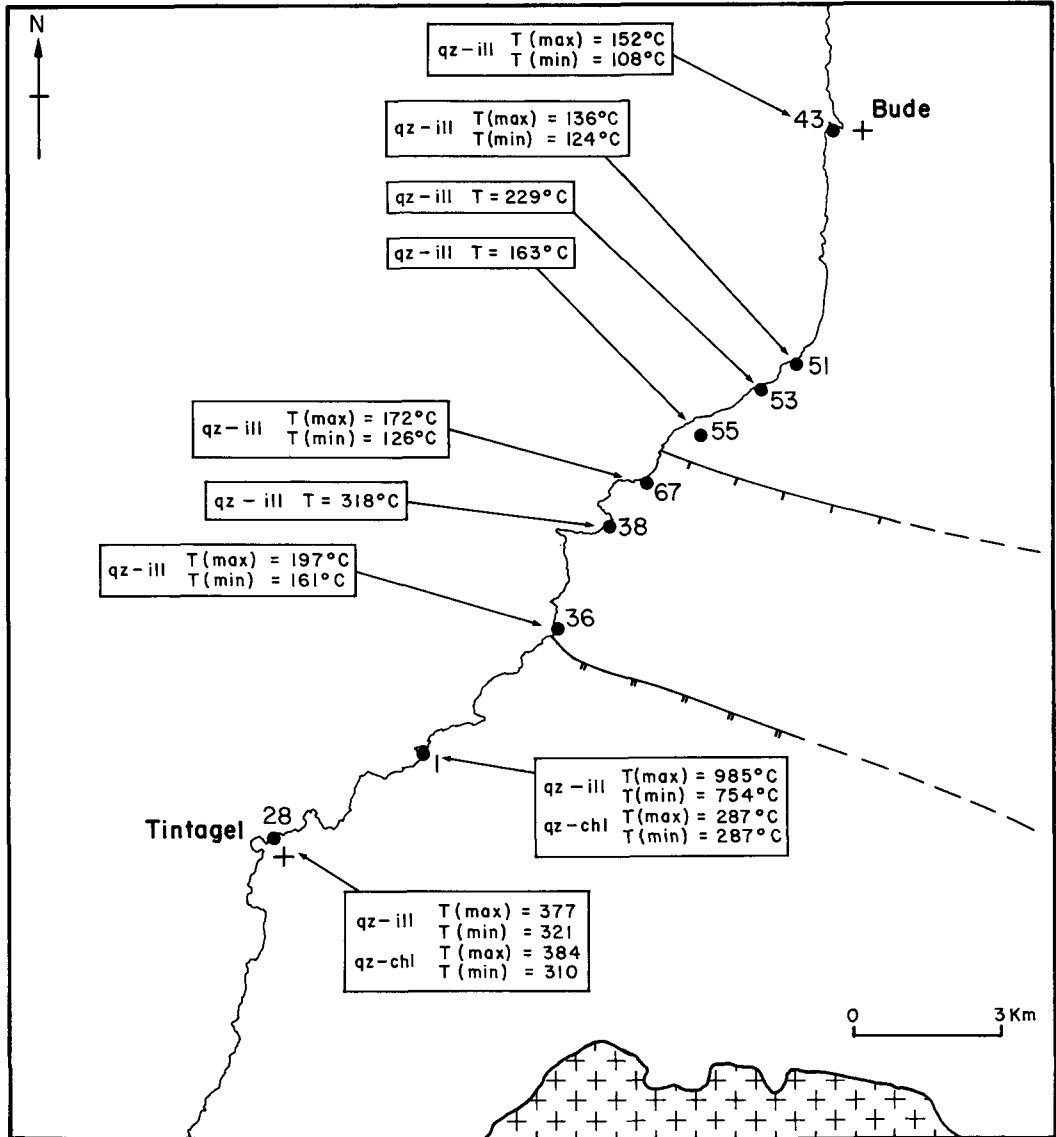
FIG. 6. Location of samples used for oxygen isotope analysis and the temperatures calculated from the geothermometers used. Also indicated are the determined illite crystallinity zones (see fig. 1).

prograde metamorphic conditions during M2 in the Tintagel district or during retrograde metamorphism of the phyllosilicates attributed to the D1/M1 event. Any variation in $\delta^{18}O$ values of the fractions analysed is due to the growth and incorporation of new material into the analysed fraction. Likewise detrital chlorite and kaolinite will be little modified by diagenetic/low-temperature metamorphism within their own stability range.

Interpretation and conclusions. A tectonic reconstruction based on a broad correlation of the temperature estimates given by the different techniques is shown in fig. 7. The section through the fold/thrust complex is based on the most recent structural interpretations (Sanderson, 1979; Shackleton *et al.*, 1982; Selwood *et al.*, 1984). Deformation began earliest in the south (Matthews, 1977) and related low-temperature metamorphism
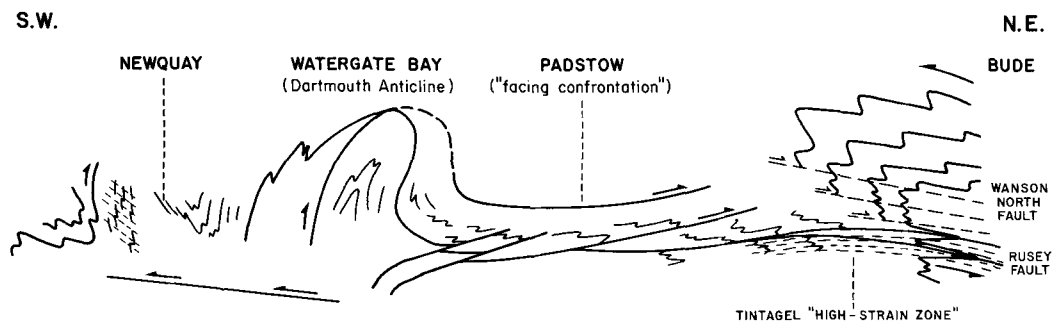
FIG. 7. Diagrammatic reconstruction (see text) representing the approximate juxtaposition of units in the complex at the peak of metamorphism in the Tintagel district (compare with fig. 3).

moved diachronously with deformation to the north throughout the Upper Carboniferous; temperatures did not exceed that of the anchizone or prehnite-pumpellyite facies ($< 275 \,°C$).

Further compression and tightening of the complex during the Westphalian resulted in the formation of a large backfold in south-west England (Shackleton *et al.*, 1982); units from greater depth and metamorphosed to a higher grade were brought up to higher structural levels. To the north and with continued northward movement during the early Permian, Upper Devonian and Lower Carboniferous sediments underthrusted the southern margin of the younger Upper Carboniferous flysch (Selwood *et al.*, 1984). Intense strain with the metamorphic grade reaching epizone/low-greenschist facies during D1, increasing to middle/upper-greenschist facies in a post-kinematic M2 phase, characterizing this zone. The Upper Carboniferous, overriding the high-strain zone along the Rusey fault was folded and heated primarily from below, the temperature regime decreasing from the base upwards. With later extension and uplift localized crystallization of retrograde metamorphic minerals in the Tintagel district occurred, overprinting the prograde mineral assemblages developed.

Although the suggested metamorphic/deformation history outlined above represents a somewhat simplified picture, it can be seen that a multidisciplinal approach such as this can be used to:

1. Show that combinations of different indicators of temperature can be usefully employed to characterize the conditions prevailing from diagenesis through to true greenschist facies metamorphism. Further work in similar types of terrain, particularly with respect to oxygen isotope geothermometry may allow, with modifications, such a method to be used in a routine fashion to help define the temperature limits of the diagenetic/low-

temperature zones described by the other indicators used (e.g. illite crystallinity etc.).

2. Apply such results obtained to the regional deformation pattern in an effort to elucidate the tectonic history of the area under consideration.

REFERENCES

Bailey, S. W. (1982) *Clay Minerals,* **17,** 243–8.
Brazier, S., Robinson, D., and Matthews, S. C. (1979) *Neues Jahrb. Geol. Palaont. Monatsh,* 641–62.
Coombs, D. S., Nakamura, Y., and Vuagnat, M. (1976) *J. Petrol.* **17,** 440–71.
Eslinger, E. V., and Savin, S. M. (1973) *Am. J. Sci.* **273,** 240–67.
—— and Yeh, H-S. (1979) In *Aspects of Diagenesis* (P. A. Scholle and P. R. Schluger, eds.). SEPM Spec. Publ. **26,** 113–24.
Ferry, J. M., and Spear, F. S. (1978) *Contrib. Mineral. Petrol.* **66,** 113–17.
Floyd, P. A. (1982) In *Igneous rocks of the British Isles* (D. S. Sutherland, ed.). Wiley.
—— and Rowbotham, G. (1982) *Proc. Ussher Soc.* **5,** 296–303.
Grainger, P., and Witte, G. (1981) Ibid. **5,** 168–78.
Guidotti, C. V., and Sassi, F. P. (1976) *Neues Jahrb. Mineral. Abh.* **127,** 97–142.
Hobson, D. M. (1976) *Proc. Ussher Soc.* **3,** 320–32.
Hutchings, W. M. (1889) *Geol. Mag.* **6,** 214–20.
Johns, W. D., and Kurzweil, H. (1979) *Tschermaks Mineral. Petr. Mitt.* **26,** 203–15.
Kisch, H. J. (1980) *J. geol. Soc. London,* **137,** 271–88.
—— (1983) In *Diagenesis in sediments and sedimentary rocks,* 2 (G. Larsen and G. V. Chillingar, eds.). Developments in Sedimentology, **25B,** Elsevier, 572 pp.

Liou, J. G. (1979) *Am. Mineral.* **64**, 1–14.

McMurty, G. M., Wang, C-H., and Yeh, H-W. (1983) *Geochim. Cosimochim. Acta*, **47**, 475–89.

Matsuhia, Y., Goldsmith, J. R., and Clayton, R. N. (1979) *Geochim. Cosimochim. Acta*, **43**, 173–82.

Matthews, S. C. (1977) *Neues Jahrb. Geol. Palaont. Abh.* **154**, 94–127.

Milliken, K. L., Land, L. S., and Loucks, R. G. (1981) *Bull. Amer. Assoc. Pet. Geol.* **65**, 1397–413.

Offler, R., Baker, C. K., and Gamble, J. (1981) *Contrib. Mineral. Petrol.* **76**, 171–6.

O'Neil, J. R., and Taylor, H. P. Jr. (1969) *J. Geophys. Res.* **74**, 6012–22.

Phillips, F. C. (1928) *Geol. Mag.* **65**, 541–56.

Pigage, L. C., and Greenwood, H. J. (1982) *Am. J. Sci.* **282**, 943–69.

Primmer, T. J. (1983) *Proc. Ussher Soc.* **5**, 421–7.

——(1984) Unpubl. Ph.D. thesis, Univ. of Bristol.

Robinson, D., and Read, D. (1981) *Proc. Ussher Soc.* **5**, 132–8.

Sanderson, D. J. (1979) *J. Struct. Geol.* **1**, 171–80.

Selwood, E. B., Thomas, J. M., and Stewart, I. J. (1984) *Proc. Geol. Assoc.* (in press).

Shackleton, R. M., Ries, A. C., and Coward, M. P. (1982) *J. geol. Soc. London*, **139**, 535–43.

Syers, J. K., Chapman, S. L., Jackson, M. L., Rex, R. W., and Clayton, R. N. (1968) *Geochim. Cosimochim. Acta*, **32**, 1022–5.

Taylor, H. P. Jr., and Coleman, R. G. (1968) *Bull. geol. Soc. Am.* **79**, 1727–56.

Tilley, C. E. (1925) *Geol. Mag.* **62**, 314–18.

Velde, B. (1977) *Clays and clay minerals in natural and synthetic systems.* Elsevier, 218 pp.

Weaver, C. E. (1960) *Bull. Amer. Assoc. Pet. Geol.* **44**, 1505–18.

Wenner, D. B., and Taylor, H. P. Jr. (1971) *Contrib. Mineral. Petrol.* **32**, 165–85.

Yeh, H-S., and Savin, S. M. (1977) *Bull. geol. Soc. Am.* **88**, 1321–30.